Quantum dots based on spin properties of semiconductor heterostructures

Manuel Valín-Rodríguez[1], Antonio Puente[1] and Llorenç Serra[1,2]

[1] *Departament de Física, Universitat de les Illes Balears, E-07122 Palma de Mallorca, Spain*

[2] *Institut Mediterrani d'Estudis Avançats IMEDEA (CSIC-UIB), E-07122 Palma de Mallorca, Spain*

(October 5, 2003)

Abstract

The possibility of a type of semiconductor quantum dots obtained by spatially modulating the spin-orbit coupling intensity in III-V heterostructures is discussed. Using the effective mass model we predict confined one-electron states having peculiar spin properties. Furthermore, from mean field calculations (local-spin-density and Hartree-Fock) we find that even two electrons could form a bound state in these dots.

PACS 73.21.La, 73.21.-b

Low-dimensional semiconductor structures constitute one of the most suitable scenarios to observe quantum phenomena in condensed matter physics. In this sense, the atomic-like properties of quantum dots and the conductance quantization in narrow wires are seminal examples widely studied [1,2]. At present, the available fabrication techniques of such semiconductor structures rely on charge-based confinement at length scales where quantum effects are unavoidable. More precisely, confinement is obtained through the energy band discontinuities of different materials or by directly creating a potential landscape by means of metallic electrodes on a semiconductor heterostructure.

The aim of this work is to point out, using a theoretical model, the feasibility of a class of mesoscopic semiconductor structures where the spin plays a relevant role in the mechanism that determines the confining properties, without being a pure spin-dependent confinement [3]. The mechanism also differs from conventional electrostatic confinement in that it does not rely on the direct coupling of the electron charge with a horizontal electric field.

In III-V non-magnetic semiconductor heterostructures there are two relevant interactions concerning the spin: the spin-orbit coupling and the hyperfine interaction between carriers and polarized nuclei. The latter mechanism has a characteristic energy scale usually lower than that of the spin-orbit coupling [3].

In semiconductors, spin-orbit coupling stems from the relativistic effect caused by the electric field due to the lack of inversion symmetry of certain alloys like III-V heterostructures. Depending on the particular origin of the electric field two contributions are distinguished; the electric field created by the bulk inversion asymmetry (BIA) of the material gives rise to the Dresselhaus term [4], while the asymmetry in the profile of the heterostructure, structural asymmetry (SIA), generates the so-called Bychkov-Rashba term [5]. This latter mechanism constitutes the basis of the proposed electronic nanostructures.

As mentioned above, the intensity of the Bychkov-Rashba spin-orbit coupling depends on the effective electric field perpendicular to the plane of the quantum well. This implies that it can be, in principle, engineered by adjusting the specific fabrication settings of each heterostructure. Another possibility to control the Rashba interaction, that has been demonstrated experimentally [6–8], is by means of an external electric field perpendicular to the plane of the quantum well.

Exploiting the tunability of the Bychkov-Rashba mechanism we consider quantum dots whose main ingredient is a space-modulated spin-orbit intensity. This spatial modulation could be obtained with biased small electrodes on top of the semiconductor heterostructure [9,10]. However, such an arrangement would not only modify the vertical electric field but it would also generate an in-plane gradient of electric potential, leading to hybrid quantum dots where both mechanisms are present: horizontal electric potential gradient and spin-orbit intensity gradient. A more refined method to obtain space modulated spin-orbit intensities requires a deeper insight in the origin of the Rashba intensity. In this respect, de Andrada *et al* [11] discussed the relevance of the barrier layers in the determination of the spin-orbit intensity. More recently, Grundler [8] has shown that for an InAs-based quantum well an applied vertical electric field of the order of 10^3 V/cm can lead to a noticeable control of the spin-orbit intensity, whereas the built-in electric field of the sample is of the order of 10^5 V/cm. This high sensitivity to a relatively weak electric field has been attributed to the induced variations in the wavefunction penetration into the barriers. The strong relevance of the barrier layers in the determination of the Rashba intensity supposes a great advantage that could help to create a quantum well having a space-modulated spin-orbit coupling through space-engineered wavefunction barrier penetration (using inhomegeneous barrier layer composition, thickness, ...). This would lead to a fixed (not tunable) substantial step in the spin-orbit intensity capable of inducing the confinement.

We model structures confining electrons from the conduction band of the semiconductor and we use the effective mass approximation. We also suppose that the motion perpendicular to the well's plane is restricted to the first transversal subband, so that the electrons effectively move in a two-dimensional region. These simplifications might be quite drastic in some cases and, therefore, the scope of this work is limited to a discussion of the feasibility of the effects rather than to a detailed quantitative description. In this model we include the standard Bychkov-Rashba term

$$\mathcal{H}_R = \frac{\lambda_R(r)}{\hbar} \left(p_y\sigma_x - p_x\sigma_y \right) \;, \tag{1}$$

where p_x and p_y represent the components of the in-plane electron's momentum and the σ's are the corresponding Pauli matrices.

In Eq. (1) the inhomogeneity of the spin-orbit intensity is included through the spatial dependence of the coupling constant $\lambda_R(r)$, which is assumed of radial type (r and θ are used to label the standard polar coordinates in the plane). To characterize the quantum dot we consider the following step-like variation of the spin-orbit intensity

$$\lambda_R(r) = \lambda_e + (\lambda_i - \lambda_e)\frac{1}{1+e^{\frac{r-R_0}{\sigma}}} \;, \tag{2}$$

where λ_e and λ_i represent the external and internal constant values of spin-orbit intensity, respectively. The quantum dot radius is given by R_0 and σ is a small diffusivity introduced to avoid discontinuities in the numerical solutions.

The Bychkov-Rashba interaction breaks the rotational symmetry of the Hamiltonian. Nevertheless, a symmetry combining spatial and spin degrees of freedom is maintained when the Rashba intensity is a purely radial function. Namely, the Hamiltonian is invariant under a combined rotation in real and spin spaces by the same angle, i.e., it commutes with the generalized angular momentum $J_z = L_z + S_z$. Note that, at variance with conventional circular quantum dots (based on electric-potential confinement [1]), the Hamiltonian no longer commutes with L_z and S_z separately. As a consequence of the J_z-symmetry the single-particle solutions can be expressed, in a general form, as two-component spinors of type

$$\mathbf{\Psi}_{nj}(r,\theta) = \begin{pmatrix} \phi_{nj\uparrow}(r)e^{i(j-1/2)\theta} \\ \phi_{nj\downarrow}(r)e^{i(j+1/2)\theta} \end{pmatrix} \;, \tag{3}$$

where n and j are quantum numbers characterizing the states, with values $n = 1, 2, \ldots$, $j = \pm 1/2, \pm 3/2, \ldots$. Since the angular parts are analytical, we can reduce the Schrödinger equation to one-dimensional radial equations for the two spinor components,

$$\begin{aligned} -\frac{\hbar^2}{2m^*}\left[\frac{\partial\phi_\uparrow}{\partial r^2} + \frac{1}{r}\frac{\partial\phi_\uparrow}{\partial r} - \frac{(j-1/2)^2}{r^2}\phi_\uparrow\right] - \lambda_R(r)\left[\frac{\partial\phi_\downarrow}{\partial r} + \frac{j+1/2}{r}\phi_\downarrow\right] &= \varepsilon_{nj}\,\phi_\uparrow \\ -\frac{\hbar^2}{2m^*}\left[\frac{\partial\phi_\downarrow}{\partial r^2} + \frac{1}{r}\frac{\partial\phi_\downarrow}{\partial r} - \frac{(j+1/2)^2}{r^2}\phi_\downarrow\right] + \lambda_R(r)\left[\frac{\partial\phi_\uparrow}{\partial r} - \frac{j-1/2}{r}\phi_\uparrow\right] &= \varepsilon_{nj}\,\phi_\downarrow \end{aligned} \tag{4}$$

where $\phi_\uparrow$ and $\phi_\downarrow$ denote $\phi_{nj\uparrow}(r)$ and $\phi_{nj\downarrow}(r)$, respectively.

The above model has been analyzed using two alternative numerical procedures: a) solving the coupled one-dimensional equations for the radial components of the eigenspinors, Eqs. (4); and b) solving the full two-dimensional problem in Cartesian coordinates, without imposing any symmetry restriction, in a uniform grid. Before discussing the numerical results it has to be noted that systems with the above spin-orbit interaction are still invariant under time reversal. Consequently, a two-fold degeneracy, known as Kramers degeneracy, must hold. From the radial equations it can easily be seen that the substitutions: $\phi_\uparrow \to \phi_\downarrow$, $\phi_\downarrow \to -\phi_\uparrow$ and $j \to -j$ lead to a new state (Kramers conjugate) with opposite generalized angular momentum and the same energy eigenvalue ($\varepsilon_{nj} = \varepsilon_{n-j}$). The expectation values $\langle S_z \rangle$ and $\langle L_z \rangle$ also change sign with the Kramers transformation. It is worth stressing that in the usual quantum dots (with an electric potential confinement of circular symmetry) the degeneracies are 4 and 2; nonzero (zero) angular momentum states being four-fold (two-fold) degenerate. Therefore, the reduction in degeneracy from 4 to at most 2 is a genuine effect of the spin-orbit interaction.

Since the spin orientation in Eq. (3) depends on the position $\mathbf{r}$, the eigenstates will show characteristic spin textures. The distribution of vertical and parallel spin read

$$
\begin{aligned}
\langle \sigma_z \rangle (r) &= |\phi_{nj\uparrow}(r)|^2 - |\phi_{nj\downarrow}(r)|^2 \\
\langle \vec{\sigma}_\parallel \rangle (r,\theta) &= 2\phi_{nj\downarrow}(r)\phi_{nj\uparrow}(r)\left[\cos(\theta)\hat{x} + \sin(\theta)\hat{y}\right] \; .
\end{aligned}
\tag{5}
$$

Note that while the vertical component is a pure radial function, the in-plane (horizontal) spin points in the radial direction. The fact that the horizontal spin follows the position vector can be easily explained from the combined rotational invariance in spin and position space: consider two points in the dot having the same radius and different azimuthal angle θ; due to the symmetry of the Hamiltonian with J_z, the local in-plane spin orientation in the second point must be that of the first point rotated the angle needed to go from the first point to the second in the real space. This property of the eigenstates is of particular interest for determining the role of the geometrical phase (Berry's phase) in mesoscopic structures [12,13].

From the numerical simulations we observe that a necessary requirement for confined states is that the spin-orbit intensity within the quantum dot must be larger than that of the outer region, i.e., $\lambda_i > \lambda_e$. The reason for this behaviour can be understood from bulk considerations: the bulk energy bands

$$
\varepsilon_{k\pm}^{\rm bulk} = \frac{\hbar^2}{2m^*}\left(k \pm \frac{m^*}{\hbar^2}\lambda_e\right)^2 - \frac{m^*}{2\hbar^2}\lambda_e^2
\tag{6}
$$

display a constant offset $-m^*\lambda_e^2/2\hbar^2$ that depends on the spin-orbit intensity (for a schematic representation of the bulk bands see Fig. 1). Therefore a bulk uniform sample with a big value of spin-orbit intensity has an energy origin for the eigenstates lower than that of a sample having a smaller intensity. In a finite system this energy mismatch can lead to bound states in the region of higher intensity. Nevertheless, it has to be noted that for each spin orientation the energy mismatch is only confining for a certain range of momenta. This means that the confining mechanism is spin-selective through the motion of the particles. In the case of circular symmetry, it implies that electrons rotating in one sense are confined if they have a given spin orientation, while electrons rotating in the opposite sense should have the opposite spin orientation to be confined.

We stress that the SO-dependent offset in Eq. (6) is the real cause of confinement since this term acts as an electrostatic potential when the SO intensity is varying in space. Actually, a different SO Hamiltonian in which this offset were not included would not lead to confined states.

Another question of relevance refers to the magnitude of the step in the spin-orbit intensity needed to obtain confined states. For a typical size of dot radius of the order of 10 atomic effective units [14] simulation shows that an intensity in the range $\lambda_i \simeq 1.5 - 2.0 \times 10^{-9}$ eVcm is required to obtain a single-particle bound state when the external intensity is zero ($\lambda_e = 0$). It is also important to specify the external value λ_e, since the minimum step required to achieve confined states strongly depends on this quantity. For instance, when the external intensity takes a value of the order of $\lambda_e \simeq 2 \times 10^{-9}$ eVcm the step needed is reduced and the required internal value is in the range $\lambda_i - \lambda_e \simeq 0.4 - 0.7 \times 10^{-9}$ eVcm.

Quantum dots satisfying the required conditions stated above show a level structure analogous to that of conventional quantum dots. For instance, a dot characterized by spin-orbit parameters in the range of the biggest Rashba intensities experimentally measured [8], $\lambda_i \simeq 4 \times 10^{-9}$ eVcm and $\lambda_e \simeq 2 \times 10^{-9}$ eVcm, shows a total of 14 single-particle bound states distributed in two subbands (see Fig. 1). The first one containing 10 states characterized by the quantum numbers $n = 1$, $j = -9/2, -7/2, \ldots, 7/2, 9/2$ and the second one having the remaining 4 states $n = 2$, $j = -3/2, -1/2, 1/2, 3/2$. Figure 2 shows the spatial representation of the lowest energy state of this dot corresponding to $n = 1, j = 1/2$ and its conjugated state $n = 1, j = -1/2$. The upper panels show the radial profile of the spinorial components for both states, the only differences between the two cases are the exchange of the spin index and the sign change in one of the components, in agreement with symmetry properties derived above. Middle panel shows the spatial distribution of the density which has radial symmetry and is common for both conjugated states. Finally, the lower panel displays the radial distribution of the S_z spin density for the two states, showing that conjugated states posses opposite spin characters.

Up to now, we have only presented results concerning the single-particle properties of the dots. There is also the possibility of the spin-orbit-based confinement to be robust against electron-electron interaction and, thus, able to support multielectron bound states. To treat the interacting problem we impose no symmetry restriction in space and we solve numerically the full two-dimensional problem including the interaction within density functional theory, using a generalization of the local-spin-density approximation (LSDA) for non-collinear spin densities (see Ref. [15] for a previous application of this formalism). Within this scheme, we find that even two-electron states can be confined to the dot. Figure 3 shows the ground state density for an interacting two-electron dot characterized by a radius of 15 units and the same spin-orbit parameters of Fig. 2. The density displays a circular ring-like shape although the spin-orbit term breaks the rotational invariance. As an additional check of this bound two-electron state, we have also solved the Hartree-Fock equations, finding a similar total energy and density distributions also confined to the dot region. Extending the calculations to treat three or more interacting electrons with the same spin-orbit term does not lead to confined states.

In summary, we have proposed a mechanism to create electronic spatial confinement based on the spin properties of III-V semiconductor structures and, more specifically, on the Bychkov-Rashba spin-orbit interaction and its strong dependence on the barrier layer composition. The eigenstates confined to these dots show common characteristics with conventional semiconductor quantum dots such as a discrete level structure of the single-particle states and the possibility of confined two-electron states. The peculiar origin of the confinement reflects in the spin properties of the single-particle eigenstates. Not any material is suitable to create this type of structures since, as stated above, Rashba spin-orbit intensities of the order 10^{-9} eVcm and a range of tunability of the same magnitude are required. In this sense, InGaAs-based wells [7] could be enough to produce the confining effect at mesoscopic scale. However, since the bulk-intensity value λ_e has a strong relevance in the determination of the minimum conditions for confinement, InAs-based wells reveal as the best candidates to fabricate these dots. This is because of their large built-in Rashba intensities, as large as 2×10^{-9} eVcm, and their tunability range of the same order [8].

This work was supported by Grant No. BFM2002-03241 from DGI (Spain).

REFERENCES

[1] L. Jacak, P. Hawrylak, A. Wójs. *Quantum Dots.* Ed. Springer (1998) p. 176.

[2] S. Datta. *Electronic transport in mesoscopic systems.* Ed. Cambridge University Press (1997) p. 373.

[3] In cases of a very high degree of nuclear polarization the pure spin-dependent confinement induced by the hyperfine inhomogeneous magnetic field also becomes important, as discussed in V. Fleurov, V.A. Ivanov, F.M. Peeters, I.D. Vagner, Physica E **14**, 361-365 (2002); Yu. V. Pershin, Phys. Rev. B, in press (cond-mat/0305002).

[4] G. Dresselhaus, Phys. Rev. **100**, 580 (1955).

[5] E. I. Rashba, Fiz. tverd. Tela (Leningrad) **2**, 1224 (1960) [Sov. Phys. Solid State **2**, 1109 (1960)].

[6] J. Nitta, T. Akazaki, H. Takayanagi and T. Enoki, Phys. Rev. Lett. **78**, 1335 (1997).

[7] C.-M. Hu, J. Nitta, T. Akazaki, H. Takayanagi, J. Osaka, P. Pfeffer and W. Zawadzki, Phys. Rev. B **60**, 7736 (1999).

[8] D. Grundler, Phys. Rev. Lett. **84**, 6074 (2000).

[9] P.W. Brouwer, J.N.H.J. Cremers, B.I. Halperin, Phys. Rev. B **65**, 081302 (2002).

[10] M. Valín-Rodríguez, A. Puente, Ll. Serra, Nanotech. **14**, 882-885 (2003).

[11] E.A. de Andrada e Silva, G.C. La Rocca, F. Bassani, Phys. Rev. B **55**, 16293 (1997).

[12] I.D. Vagner, A.S. Rozhavsky, P. Wyder, A. Yu. Zyuzin, Phys. Rev. Lett. **80**, 2417 (1998).

[13] A.G. Aronov, Y.B. Lyanda-Geller, Phys. Rev. Lett. **70**, 343 (1993).

[14] Atomic effective units take values in the range of 10-50 nm for distance (a_0^*) and 5-10 meV for energy (H^*), using typical semiconductor parameters, while atomic effective units of spin-orbit intensity are more homogeneus for the different materials having a good approximate value of 1×10^{-8} eVcm.

[15] M. Valín-Rodríguez, A. Puente, Ll. Serra, Phys. Rev. B **66**, 045317 (2002).

FIGURES

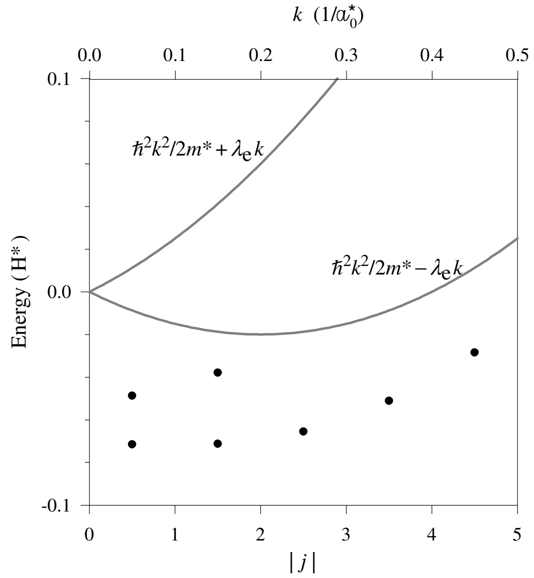

FIG. 1. Structure of the bound states as a function of the generalized angular momentum j for a quantum dot having $\lambda_e = 0.2\, H^* a_0^* \simeq 2 \times 10^{-9}$ eVcm, $\lambda_i = 0.4\, H^* a_0^* \simeq 4 \times 10^{-9}$ eVcm and a nominal dot radius $R_0 = 10$ effective atomic units (lower scale). Solid lines represent the bulk bands corresponding to the surrounding material characterized by λ_e (upper scale).

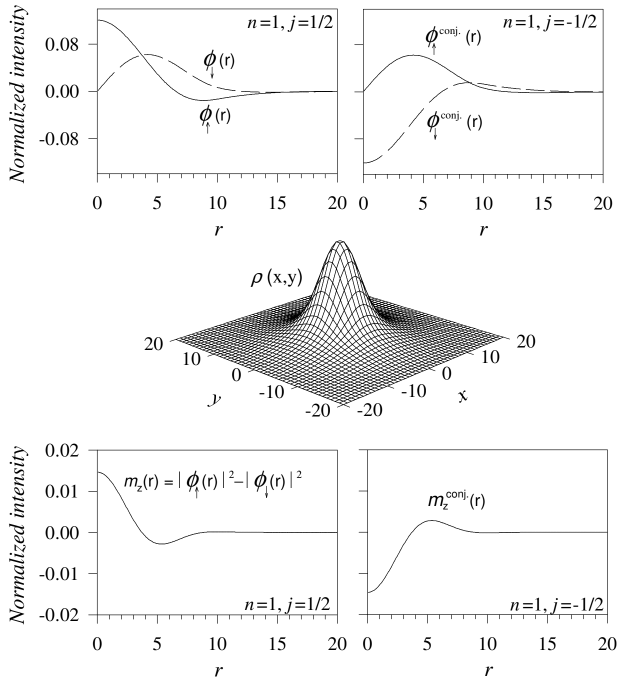

FIG. 2. Upper panels: radial spinorial components corresponding to the lowest energy pair of conjugated states. Middle panel: two-dimensional representation of the probability density corresponding to the above Kramers conjugated states. Lower panels: radial profile of the σ_z spin density distribution corresponding to the same conjugated states. All coordinates are expressed in terms of atomic effective units of distance

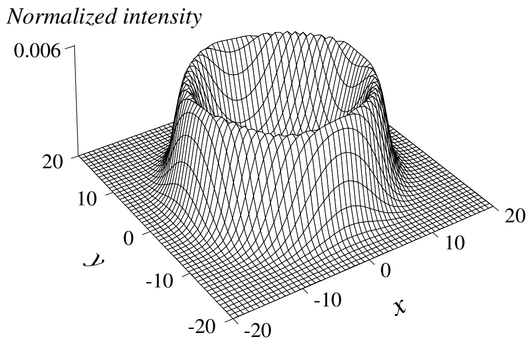

FIG. 3. Two-dimensional representation of the LSDA density corresponding to an interacting two-electron dot characterized by $\lambda_e = 0.2\,H^* a_0^* \simeq 2 \times 10^{-9}$ eVcm, $\lambda_i = 0.4\,H^* a_0^* \simeq 4 \times 10^{-9}$ eVcm and a dot radius of 15 units. Atomic effective units of distance are used to represent the Cartesian coordinates.